Transient thermal response in ultrasonic additive manufacturing of aluminum 3003

David Schick
Welding Engineering, The Ohio State University, Columbus, Ohio, USA

Sudarsanam Suresh Babu
Materials Science and Engineering, The Ohio State University, Columbus, Ohio, USA

Daniel R. Foster and Marcelo Dapino
Mechanical Engineering, The Ohio State University, Columbus, Ohio, USA

Matt Short
Ultrasonics, Edison Welding Institute, Columbus, Ohio, USA, and

John C. Lippold
Welding Engineering, The Ohio State University, Columbus, Ohio, USA

Abstract

Purpose – Ultrasonic additive manufacturing (UAM) is a rapid prototyping process through which multiple thin layers of material are sequentially ultrasonically welded together to form a finished part. While previous research into the peak temperatures experienced during UAM have been documented, a thorough examination of the heating and cooling curves has not been conducted to date.

Design/methodology/approach – For this study, UAM weldments made from aluminum 3003-H18 tapes with embedded Type-K thermocouples were examined. Finite element modeling was used to compare the theoretical thermal diffusion rates during heating to the observed heating patterns. A model was used to calculate the effective thermal diffusivity of the UAM build on cooling based on the observed cooling curves and curve fitting analysis.

Findings – Embedded thermocouple data revealed simultaneous temperature increases throughout all interfaces of the UAM build directly beneath the sonotrode. Modeling of the heating curves revealed a delay of at least 0.5 seconds should have existed if heating of lower interfaces was a result of thermal diffusion alone. As this is not the case, it was concluded that ultrasonic energy is absorbed and converted to heat at every interface beneath the sonotrode. The calculated thermal diffusivity of the build on cooling was less than 1 percent of the reported values of bulk aluminum, suggesting that voids and oxides along interfaces throughout the build may be inhibiting thermal diffusion through thermal contact resistance across the interface.

Originality/value – This work systematically analyzed the thermal profiles that develop during the UAM process. The simultaneous heating phenomenon presented here has not been documented by other research programs. The findings presented here will enable future researchers to develop more accurate models of the UAM process, potentially leading to improved UAM bond quality.

Keywords Ultrasonics, Additive manufacturing, Thermocouples, Metals, Heat transfer

Paper type Research paper

1. Introduction

Ultrasonic additive manufacturing (UAM) or ultrasonic consolidation is a solid state welding process in which thin foil layers are ultrasonically welded on top of one another and computer numerical control machined to create a final part. The substrate is preheated and significant normal forces are applied to aid in the joining process. The exact mechanism for joining is not fully understood, though it is believed to be similar to forge welding, with significant plastic flow of material and no melting. As this process is completely solid state, it offers many benefits over traditional arc welding processes. This includes allowing for complex shapes and designs, having a significantly lower processing temperature, allowing for embedded materials and channels, and joining material combinations that are otherwise difficult or impossible (Janaki Ram *et al.*, 2007).

At the beginning of each sequence, a new foil is placed on top of the previous layers by a feed roll. The new foil is then tacked down to the previous layers through a tacking pass. This pass is made at relatively low normal forces (200-400 N), low amplitude (8-12 μm), and high travel speed (50-80 mm/s). Initially, the asperities on the surfaces of the two materials come in contact and through ultrasonic

The current issue and full text archive of this journal is available at **www.emeraldinsight.com/1355-2546.htm**

Rapid Prototyping Journal
17/5 (2011) 369–379

[DOI 10.1108/13552541111156496]

The authors would like to thank the Cooperative Research Program of Edison Welding Institute for supporting this research. In addition, they thank Dr K. Graff (Edison Welding Institute (EWI)) and Dr M. Sriram (Ohio State University (OSU)) for suggestions and fruitful discussion during preparation of the manuscript.

Received: 7 February 2010
Revised: 24 March 2010
Accepted: 25 March 2010

vibration, may be sheared off or plastically deformed. At the end of the tacking pass, the materials are lightly bonded together. To complete the joining process, a welding pass with higher ultrasonic energy input (higher amplitude of vibration, higher normal forces, and slower travel speed) is made. During processing, the rough sonotrode texture is transfered to the top of the layer being added. This then becomes the bottom of the next interface, creating a situation where the top of each interface is relatively smooth while the bottom is highly textured. Johnson (2008) has suggested that this arrangement of different surface finishes is the cause of the voids found along the interfaces. Residual voids occur because some deep troughs cut by the sonotrode in the bottom half of the interface are too large to be filled in by local plastic flow.

It is believed that during UAM, some of the ultrasonic energy is dispersed in the material by the formation of vacancies and dislocations. Gunduz *et al.* (2005) calculated vacancies were on the order of 10 per cent of lattice sites, much higher than the 10^{-6} values found in aluminum at 149°C (Hatch, 1984). This high-level of vacancies may partially account for the level of plastic flow observed in UAM weldments and enables the rough and smooth surfaces to come together and be successfully bonded. The plastic flow also allows for the embedding of fibers and other small materials between two layers (Janaki Ram *et al.*, 2007; Li and Soar, 2008; Yang *et al.*, 2007). In the area immediately surrounding an embedded fiber, there appears to be a decrease in the void concentration. This area also often exhibits subgrain refinement and an increase the hardness, most likely due to the high stress and plastic flow levels caused by the added material of the fiber (Yang *et al.*, 2007; Li and Soar, 2008).

Research into temperatures reached during ultrasonic spot welding (USW) has been ongoing since the 1950s. Hazlett and Ambekar (1970) used thermocouples embedded in ultrasonic spot welds to record the average maximum temperature of the spot weld withdifferent processing parameters and materials. Their work on iron-constantan (55 Cu-45 Ni) and copper-constantan spot welds revealed that if a minimum temperature (163-174°C) was reached during welding, the sample would fail outside of the weld region indicating a good weld. Cross sections examined under optical and scanning electron microscopes revealed minimal diffusion, leading to the conclusion that the bonding mechanism was mechanical or metallurgical due to nascent surface creation. Working on materials with a natural thermocouple, copper and monel (an alloy of 65-70 per cent nickel and 20-29 per cent copper with some iron and manganese additions), Weare *et al.* (1960) recorded temperatures up to 232°C. Using a plate of glass between the welding tip and anvil, they were able to visually observe hot spots of near 1,400°C in molybdenum samples, the temperature required to emit the white light. Red and white light was observed in copper and aluminum samples, indicating temperatures above 520°C. This indicates that while natural thermocouple readings may level out, temperatures may continue to rise at some locations within an ultrasonic spot weld. In the study, dedicated thermocouples with a larger operating range were used to overcome this issue. More recent research by de Vries (2004) on aluminum 6061-T6 ultrasonic spot welds recorded temperatures up to 220°C using an infrared camera with a reported accuracy of ±10°C. He also found that the weld heated extremely fast, reaching 200°C within 40 ms (5,000°C/s). Finally, de Vries found a link between higher welding temperatures and heavy plastic deformation of the spot weld, illustrating the importance of obtaining accurate temperature measurements for UAM.

While USW is similar to UAM, the transient nature of UAM compared to the static nature of USW results in significant differences in operating conditions, including temperatures. Kong *et al.* (2004b) embedded Type-K thermocouples in UAM builds made from aluminum alloy 3003-H18 with NiTi shape memory alloy fibers. The goal of their use of thermocouples was to test for the maximum temperature reached during the embedding process. At the highest amplitude (14.3 μm), highest normal force (276 kPa), and lowest travel speed (27.8 mm/s), the maximum temperature recorded was 150°C. Lower energy build parameters resulted in maximum temperatures of less than 70°C, with an almost linear correlation between amplitude of vibration and maximum temperature. Yang *et al.* (2009) also embedded Type-K thermocouples in aluminum alloy 3003-H18 foils and recorded peak temperatures between 68 and 98°C, depending on process parameters (10-12 μm amplitude and 206-275 kPa normalforce). Both Kong's *et al.* (2004b) and Yang's *et al.* (2009), thermocouple research were conducted at Loughborough University using the same ultrasonic seam welder. It is difficult to directly compare the values obtained in the study, as both Kong and Yang did not use preheat and due to machine setup differences, set and reported normal forces differently. In the present research, six thermocouples were embedded in each build and the entire heating and cooling process was analyzed for both tacking and welding passes.

2. Experimental procedures

2.1 Materials

In this research, a non-age hardenable Al-3003 (Al-1 Mn-0.7 Fe-0.12 Cu wt. per cent) alloy was used as both tapes (H18 fully strain hardened, 150 μm thick, 25.4 mm wide) and substrate (H14 partially strain-hardened, over 25.4 mm thick). The composition of the materials used meets the standard specification of the alloy, nominally Al-1.3 Mn-0.7 Fe-0.1 Cu.

2.2 UAM build parameters

A total of five builds were made, three block type builds and two step type builds. The processing parameters for the builds are shown in Tables I and II. The position of thermocouples and build layouts are shown schematically in Figure 1. For the step builds, all of the thermocouples were installed at the same time. In the block builds, the process was paused to install a thermocouple every ten layers. Data were recorded for the subsequent foil layer that was deposited directly on top of the thermocouples. The block builds were used to determine the effect of subsequent passes on lower interfaces and to determine the rate at which the interfaces

Table I UAM block build parameters

Pass	Force (N)	Rate (mm/s)	Amplitude (μm)
Tacking	300	59.27	14
Welding	750	50.4	24

Table II UAM step build parameters

Pass	Force (N)	Rate (mm/s)	Amplitude (μm)
Tacking	300	59.27	14
Welding	700	50.4	24

cooled back to the preheat temperature. Conversely, the step builds were used to verify the results of the block builds and to check for any potential problems with the thermocouples or the recording setup. The focus of this research program was on the results obtained from the block builds.

2.3 Thermocouple data and analysis

Type K thermocouples, 127 μm in diameter (36 AWG), were embedded between UAM layers. The temperatures were recorded at a rate of 10,000 Hz per channel. The data were converted to Excel™ files and analyzed with Igor Prork using a custom macro file. The macro file found the minimum and maximum temperatures recorded, maximum instantaneous heating and cooling rates, average heating rate during the upwards peak, and the time temperatures of interest were reached. A cooling curve analysis was done based on the cladding equation with a 2d heat transfer with a distributed heat source see equation (1) (Grong, 1997). This generated an effective thermal diffusivity of the UAM build given as a percentage of aluminum 3003:

$$T - T_0 = \left(\frac{q_0/2vL}{\rho c\sqrt{\pi}}\right)\left(\frac{exp(-z^2\sqrt{4at})}{\sqrt{4at}}\right) \times \left(erf\left(\frac{y+L}{\sqrt{4at}}\right) - erf\left(\frac{y-L}{\sqrt{4at}}\right)\right) \quad (1)$$

In equation (1), T is the temperature (K) at the point and time of interest, while T_0 is the preheat temperature (338 K). The calculated heat generated is q_0 (averaged 60-100 watts), v is the travel speed (50.8 mm/s), and L is half the length of the distributed heat source (20 mm). The material properties are density ($\rho = 0.0027$ g/mm^3) and specific heat ($c = 1\,J\,g^{-1}\,°C^{-1}$). Z is the distance in the depth direction from the heat source where the temperature is desired (0 in this case). The time, t was calculated based on the travel speed. The thermal diffusivity is in the "a" parameter, which in this case was 85 mm^2/s times a multiplier. The multiplier is the effective thermal diffusivity that was solved for, so a multiplier value of 1 would indicate the cooling occurred at the same rate as a solid block of aluminum while values below 1 indicate slower than expected cooling occurred. This equation was used as it most accurately described the situation of UAM, a moving, distributed heat source that extends the complete width of the part being welded.

2.4 Temperature rise and thermal diffusion calculations

In addition to cooling curve analysis, elementary calculations were performed to estimate the expected rise in temperature based on the operating conditions and material properties of aluminum (equation (2)). The parameters used for equation (2) are presented in Table III:

$$\Delta T = \frac{\text{Energy (Joules)}}{\text{Mass (Grams)} \times \text{Specific Heat (J/gm} \cdot \text{K)}} \quad (2)$$

In order to compare the time of the peak temperatures from the block builds, a finite element model (FEA) was produced in Ansys™. A 2d solid block with the material properties of aluminum 3003 (thermal conductivity = 0.2295 W mm^{-1} °C^{-1}, specific heat = 1 J g^{-1} °C^{-1}, density = 0.0027 g/mm^3) with dimensions of 50 mm wide by 8 mm tall was used. A stationary heat source was centered on the top, held at 150°C, and was 5 mm wide. A mesh size of 0.3 mm was used throughout and a time step of 0.01 seconds was used. For visual purposes, a temperature rang of 65-95°C was used, any temperatures above 95°C were gray. This allowed for determination of the time delay before various depths of the build reached 95°C.

2.5 Solid block thermocouple control experiment

A control experiment to determine if the ultrasonics or normal forces affected the results of the block build was performed. A solid aluminum 3003 block was cast with six thermocouples installed, however, two were fractured during installation or handling and could not be used. The block was 203 mm long and 25.4 mm wide, a similar size and shape of the UAM block

Figure 1 Thermocouple configuration for the block and step builds

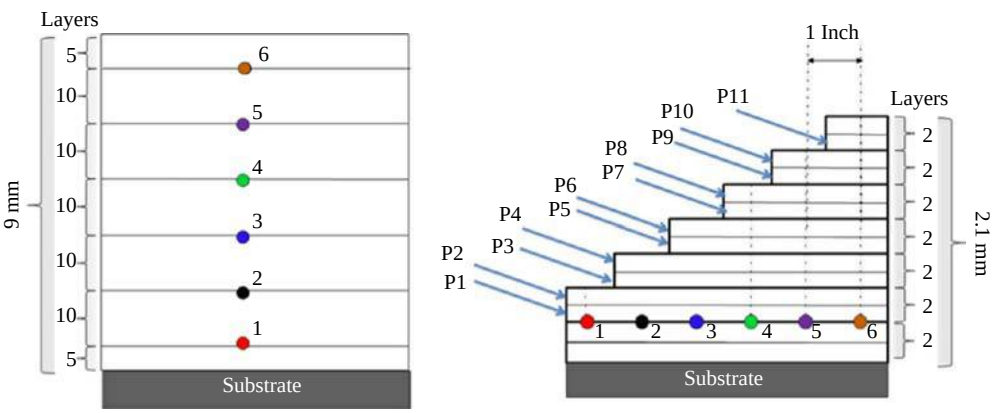

(a) Block build **(b)** Step build

Notes: (a) Thermocouple locations in block builds; the thermocouples were placed approximately half way in the build length direction; (b) thermocouple locations in the step builds

Table III Parameters used for temperature rise calculations

Parameter	Setting	Units
Power input	3,000	Watts
Travel speed	42.33	mm/s
Tape width	25.4	mm
Tape height	0.30	mm
Tape length	4	mm
Tape volume	30.48	mm^3

setup. Thermocouples were stacked vertically with a goal of 1.5 mm between them, however, during casting the thermocouples moved slightly, resulting in the following positions (from the top surface): 1.93, 2.19, 3.64 and 5.19 mm, see Figure 2 for a schematic of the final arrangement. The sample was mounted in the same UAM machine used for the other builds and four tacking and welding passes were performed at the same operating parameters as the block builds (Table II). The thermocouple data were recorded, exported to Excel™ and analyzed with Igor Pro™ in the same manner as the other thermocouple data.

3. Results and discussion

3.1 Thermocouple data

3.1.1 Block build data

After analyzing the thermocouple data, it was clear that most of the data followed similar patterns (Figure 3). In the tacking passes the thermocouple initially reports a temperature near the preheat temperature (55-65°C), as it is simply resting on the surface of the build. As the sonotrode approaches the newly added foil (at room temperature) is gradually forced into thermal contact with the thermocouple and the lower layer, causing a drop in preheat temperature at the thermocouple to be recorded as the cold foil layer absorbs the heat. When the sonotrode is directly on top of the thermocouple, the ultrasonic energy is dissipated at the interface causing a sharp rise in temperature. The area then cools slowly through conductive and convective cooling.

Figure 2 Schematic of the setup used for the solid aluminum block confirmation experiment

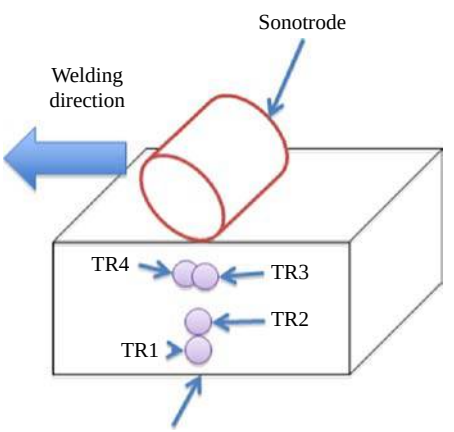

Note: The thermocouples (in reverse order) were 1.93, 2.19, 3.64 and 5.19mm from the top surface

The welding passes were similar, except in most cases there was no cooling before the peak as the new layer was at the preheat temperature as well. Welding passes generally exhibited higher peak temperatures than tacking passes, often by 30-60°C. This was expected due to the higher levels of ultrasonic power input during the welding passes. On the 149°C preheat block builds, the temperature spike for the tacking passes is not easily seen, as the level of undercooling before the spike ranged up to 90°C. This result is also easily explained due to the large temperature difference (149 versus 22°C) between the lower layer and the new, "cold", foil layer.

3.1.2 Step build data

The thermocouple data from the step builds were similar to the block build, with the first tacking passes exhibiting slight precooling, and earlier welding passes generating more heat than later passes. The temperature peaks were evenly spaced at 0.5 seconds apart, which coincides with the 50.8 mm/s travel speed and 25.4 mm spacing between thermocouples. Thermocouples that were not directly welded over during later passes did not report any significant temperature rises above the preheat temperature. This indicates there is no ultrasonic preheating, and the ultrasonic energy is directed down only, not laterally along the interface.

3.1.3 Block build peak temperature data

The first welding pass on top of each thermocouple reached the highest temperatures (Figure 4). The average maximum temperatures for the first tacking pass for the 65°C preheat block build was 89°C. The first welding passes averaged a peak temperature 146°C. The second welding pass over the thermocouple generally resulted in the second highest maximum temperature, with an average of 101°C. During subsequent passes the average peak temperature continued to progressively drop (Table IV). For the 149°C preheat block build, the average peak temperature for the first tacking pass was 137°C and the first welding pass was 168°C. Subsequent welding passes yielded average peak temperatures between 146 and 152°C.

3.1.4 Instantaneous heating and cooling rates

The average maximum instantaneous heating rates (Figure 5) were calculated for the 65°C block build to be 1,250°C/s for the first tacking pass and 2,221°C/s for the first welding pass. For the 149°C preheat builds, the average maximum instantaneous heating rate was 1,450°C/s for the first tacking pass and 1,398°C/s for the first welding pass. The average maximum instantaneous cooling rates (Figure 6) were 687°C/s and 1,343°C/s for the 65°C preheat tacking and welding passes, respectively. The average cooling rates for the 149°C preheat builds were 1,381 and 780°C/s for the tacking and welding passes, respectively. In later passes, the maximum heating and cooling rates trend slowly lower, though they appear to level off around 500°C/s after many layers. Thermocouples 2 and 4 from the 149°C preheat build did not yield consistent results and brought the average maximum heating and cooling rates down considerably. Without thermocouples 2 and 4, the average maximum heating and cooling rates were 1,850 and 976°C/s, respectively.

3.2 Thermocouple data patterns

Analysis of the thermocouple data revealed three distinct patterns. These have been designated:

1 normal heating and cooling;

Figure 3 Tacking and welding temperature results, example thermocouple data from both preheat conditions block builds

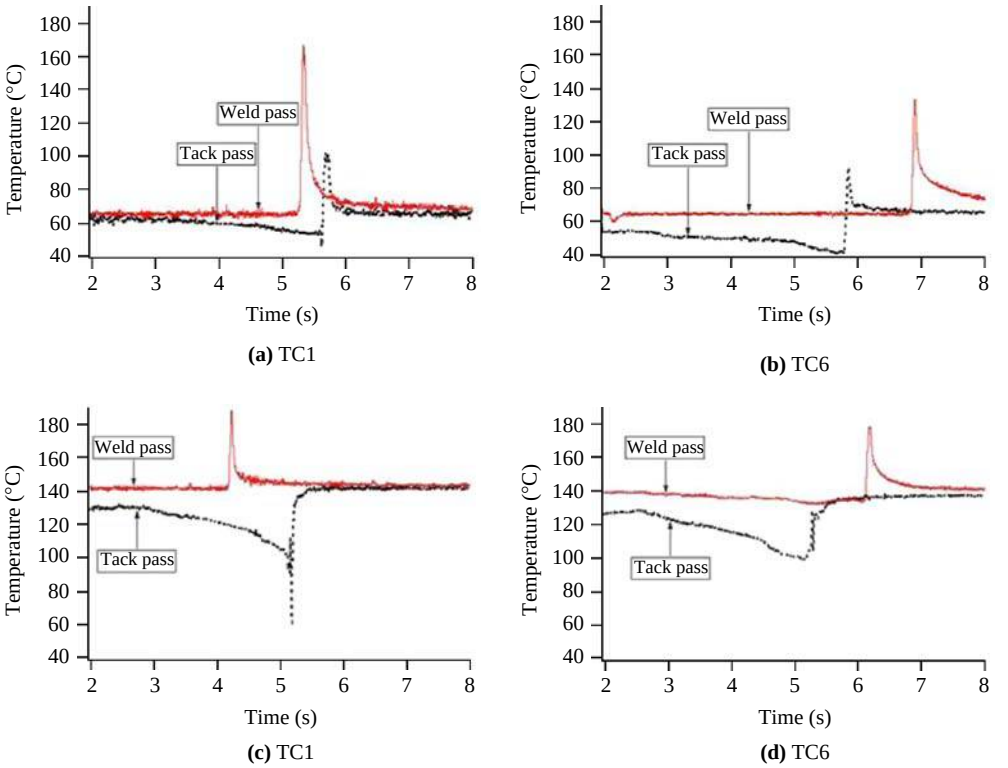

(a) TC1 **(b)** TC6 **(c)** TC1 **(d)** TC6

Notes: (a) Thermocouple 1, 658C preheat; (b) thermocouple 6, 658C preheat; (c) thermocouple 1, 1498C preheat; (d) thermocouple 6, 1498C preheat; the difference in time between the peaks of the tacking and welding passes is due to when the recorder was started relative to the beginning of the pass

Figure 4 Maximum temperature recorded during the welding passes, (a) 65°C and (b) 149°C preheat block builds

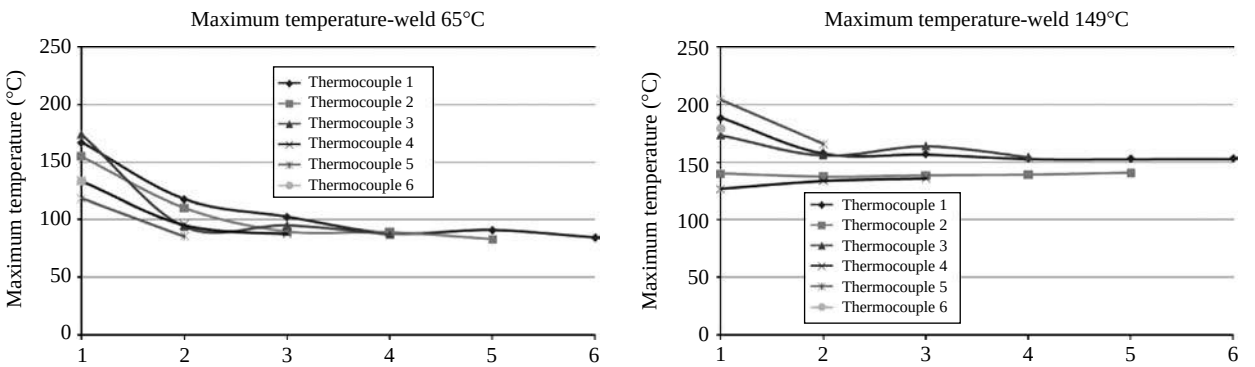

(a) Welding pass number (after thermocouple installed) **(b)** Welding pass number (after thermocouple installed)

Note: The highest temperatures were recorded during the first welding pass after the thermocouple was installed indicating most of the ultrasonic energy is absorbed at the topmost interface

2 gradual cooling followed by normal heating and cooling; and
3 gradual cooling followed by gradual heating.

A mechanism has been developed to explain these three situations.

3.2.1 Normal heating and cooling

Normal heating and cooling patterns were found on the weld passes of most of the 65°C preheat block build passes and some of the weld passes of the 149°C preheat block build passes. In this situation, the new layer has already been tacked down and is in intimate thermal contact with the substrate material below. When the sonotrode approaches, the ultrasonic energy is directed to the interface, which then heats up due to a combination of frictional and deformational heating. Once the sonotrode has passed, slow cooling occurs as the heat diffuses away into the surrounding material. This results in the familiar and expected heating and cooling pattern.

Table IV Average peak temperature versus passes since embedded for 65°C preheat block build

Passes	Average maximum temperature (°C)
1	146.7
10	100.6
20	93.8
30	88.2
40	86.9
50	84.6

3.2.2 Gradual cooling followed by normal heating and cooling
This situation occurred on most tacking passes in both of the block builds. In the 65°C preheat builds, this was limited to the top most thermocouple when the new "cold" foil layer was being added, while in the 149°C builds this occurred with many of the thermocouples during all tacking passes. In this situation, the area surrounding the thermocouple is cooled before the sonotrode arrives, at which point, it follows a normal heating and cooling pattern. The cause of the precooling in most cases is the new foil layer being added is at room temperature, far below the preheat temperature. When the sonotrode approaches the thermocouple location, the new foil is gradually brought into thermal contact with the lower layers, causing a drop in local temperature as observed by the thermocouples. When the sonotrode is directly on top of the thermocouple, an instant spike in temperature is observed as the local vibrations at the interface cause a rise in temperature of the material surrounding the thermocouple.

3.2.3. Gradual cooling followed by gradual heating
Gradual cooling and heating occurred only in the 149°C preheat builds. It was prominent in thermocouples 2 and 4 for the 149°C preheat block build (Figure 7). In some cases, such as 149°C TC4, this pattern existed for all passes, while in other cases, such as 149°C TC2, this pattern existed only on passes subsequent to when the thermocouple was first embedded. It is possible that due to significant voids near the thermocouple, the layer above the thermocouple is actually cooled to below the preheat temperature. This is possible as only the substrate is kept at the preheat temperature, the upper portion of the build may be significantly cooler. When the sonotrode approaches, the top layer is compressed down onto the thermocouple, removing heat from it. Thermal contact resistance (Grujicic *et al.*, 2005), due to the voids and oxides along the interfaces, may be the cause of this temperature differential. This would result in a gradual cooling as the sonotrode presses the foil layers above and below the thermocouple into thermal contact. Once the sonotrode passes over, the thermal contact resistance between the layers increases again and the thermocouple is gradually brought back to the preheat temperature by the foil layer beneath it. Large voids may also prohibit relative motion between the layers, limiting or eliminating local frictional and deformational heating.

3.3 Simultaneous heating

During all tacking and welding passes of the block builds, a phenomenon was observed. All of the thermocouples observed a spike in temperature at almost the same time, see the data as plotted by Igor Pro™ in Figure 8. If all of the ultrasonic energy were absorbed at the topmost interface, there should be a time delay due to thermal diffusion between the temperature peaks of the different thermocouples. Since this is not the case, there must be local heating along each interface as the sonotrode passes over. During each recorded welding passes the lower thermocouples displayed very similar peak temperature values. As the build height increased, the average peak temperature of the lower thermocouples decreased (Table III). As the ultrasonic energy is dispersed over a larger area, lower peak temperatures would be expected.

In order to quantify the expected delay from thermal diffusion between peak temperatures at the different thermocouple build locations, a FEA was created in Ansys™. A stationary, 5 mm wide, 150°C heat source was positioned in the center, and the progression of the 95°C isotherm was plotted (Figure 9). The upper thermocouples should have reached their peak temperature only 0.06 seconds after the top thermocouple, which is within the margin of error of the thermocouple measurements. However, the bottom thermocouple, which was 8 mm from the top, should have not reached peak temperature until 0.51 seconds after the top thermocouple. This result was confirmed by using the basic diffusion equation (equation 3). A minimum time of 0.19 seconds would be required for any thermal energy to diffuse from the top of the build to the bottom

Figure 5 Maximum instantaneous heating rate recorded during the welding passes, (a) 65°C and (b) 149°C preheat block builds

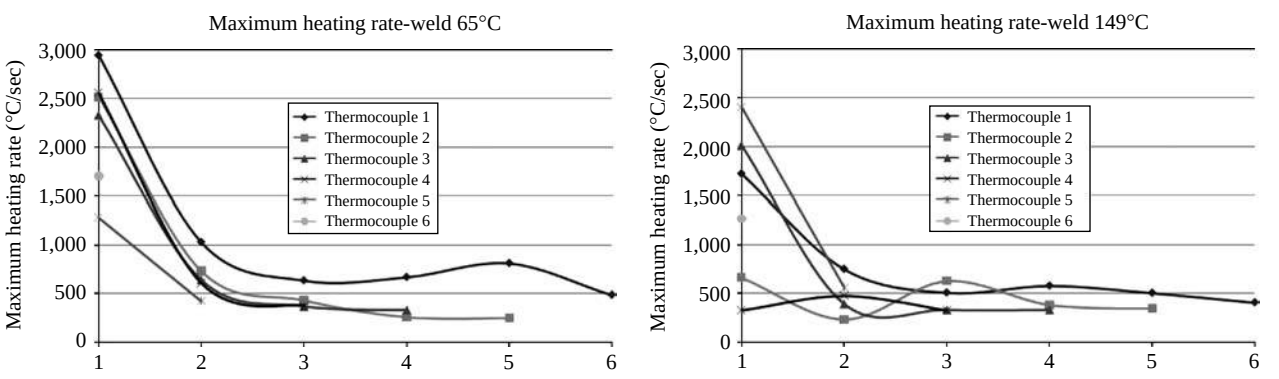

(a) Welding pass number (after thermocouple installed)

(b) Welding pass number (after thermocouple installed)

Note: The highest heating rates were recorded during the first welding pass after the thermocouple was installed indicating most of the ultrasonic energy is absorbed at the topmost interface

Figure 6 Maximum instantaneous cooling rate recorded during the welding passes, (a) 65°C and (b) 149°C preheat block builds

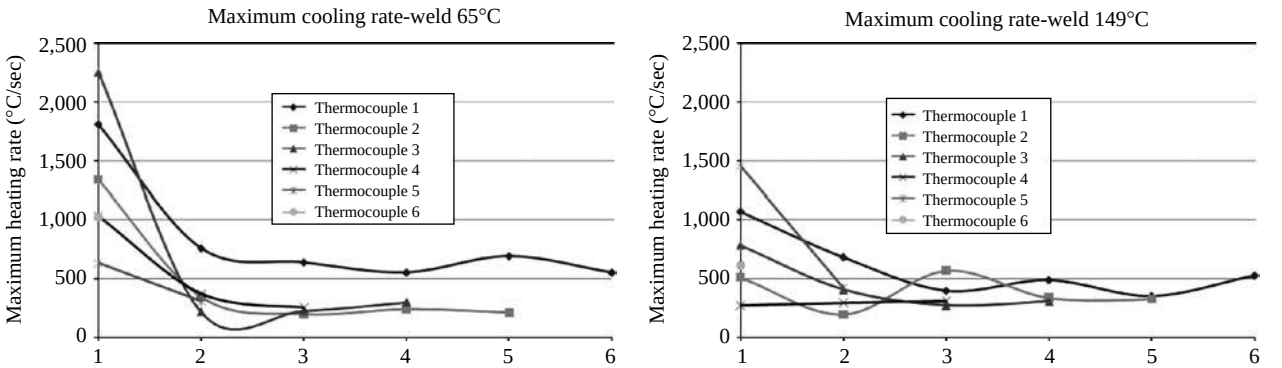

(a) Welding pass number (after thermocouple installed) **(b)** Welding pass number (after thermocouple installed)

Note: The highest temperature drops were recorded during the first welding pass after the thermocouple was installed

Figure 7 Thermocouple data from the 149°C preheat build

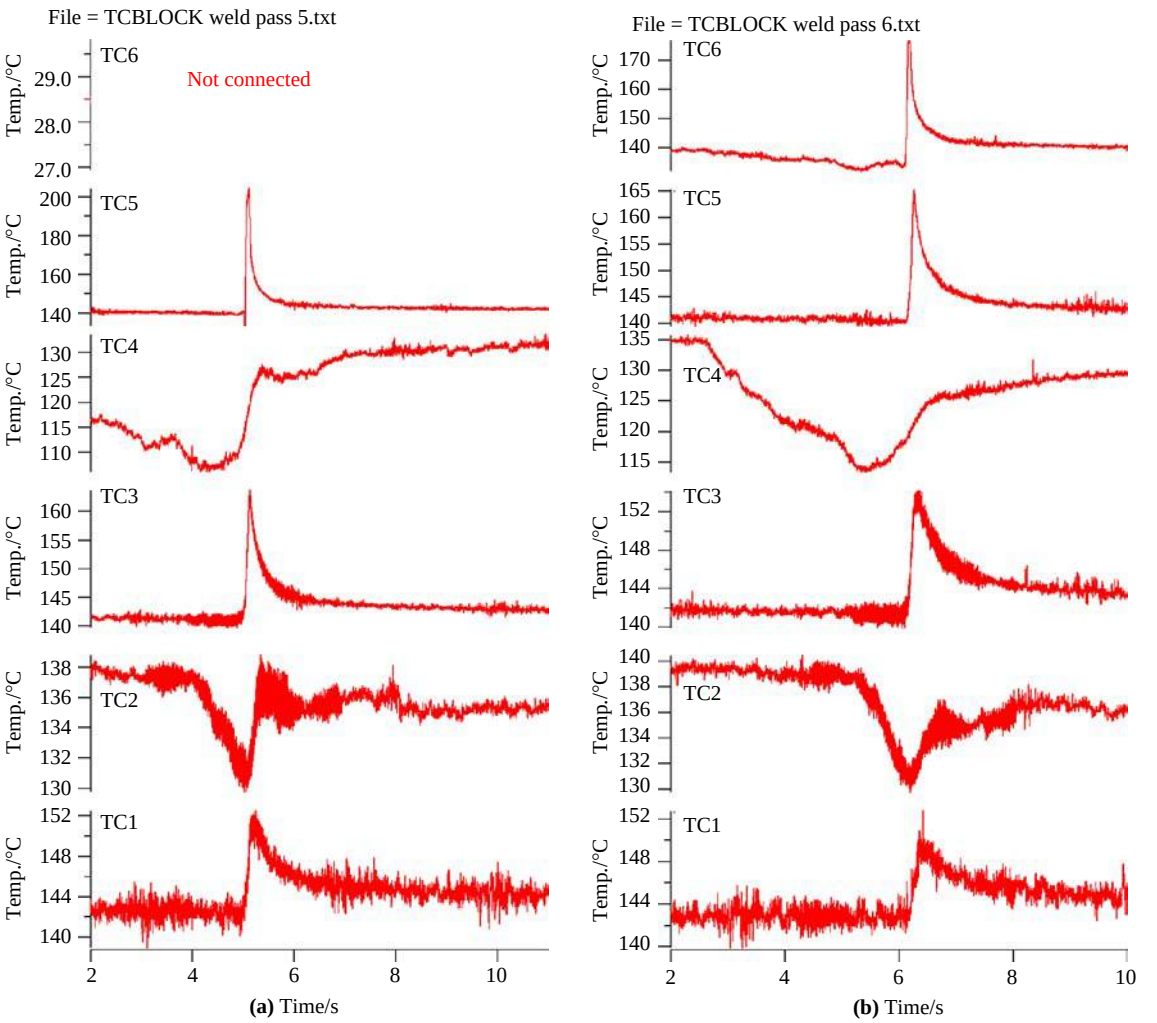

(a) Time/s **(b)** Time/s

Notes: (a) Welding pass 5, and (b) welding pass 6; thermocouples 1, 3, 5, and 6 all followed normal heating and cooling patterns, while thermocouples 2 and 4 followed gradual cooling followed by gradual heating patterns

Figure 8 Temperature data from welding pass 6, 65°C block build

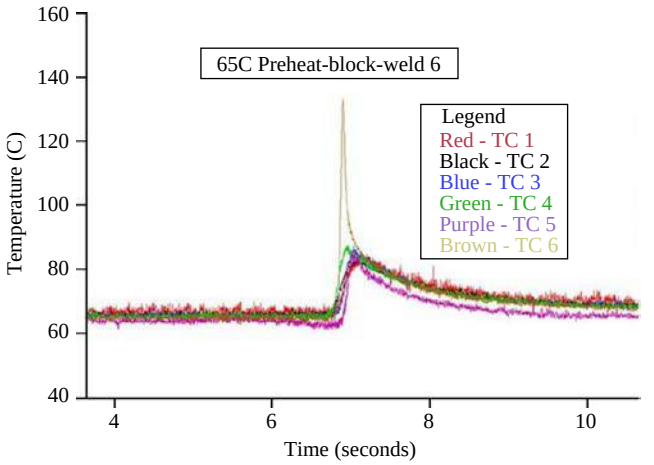

Notes: All of the lower thermocouples report a temperature spike at the same time as the topmost thermocouple: this indicates local heating along all interfaces, not just the topmost interface; lower thermocouples all show maximum temperatures around 90°C

of the build. This delay was not observed, indicating local heating must be occurring at every interface:

$$X = 2 \times \sqrt{Dt} \tag{3}$$

$$8\,mm = 2 \times \sqrt{85\,mm^2/s \times t} \tag{4}$$

$$t = 0.19\ \ seconds \tag{5}$$

The mechanism by which ultrasonic energy is absorbed and converted to heat at every interface is unknown, and could be either frictional or deformational heating or a combination of both. This may indicate the bond made during previous passes may be broken and reformed during subsequent passes if sufficient ultrasonic energy is used. Furthermore, this may account for the leveling off, or even negative returns, of peel tests found by other researchers when increasing the ultrasonic energy input into the system (Yang *et al.*, 2007; Kong *et al.*, 2004a). The previous temperature studies on UAM did not use stacked thermocouples, preventing this phenomenon from being discovered. This simultaneous heating finding was unexpected, and further study of this phenomenon may prove useful in attempts to understand and model the UAM process.

3.4. Ultrasonic stress-strain field

In many of the welding passes, lower thermocouples begin heating up slightly before upper thermocouples. The time at which each thermocouple reported the peak of the temperature spike for the 65°C block build weld pass 5 is shown in Figure 10. If heat was only generated at the topmost interface, the actual plot would have matched the expected plot generated with FEA modeling, with lower thermocouples having a longer delay before the peak temperature. Instead, the actual plot is nearly flat indicating simultaneous heating occurred. This suggests an ultrasonic stress-strain field may be occurring (Figure 11). The authors theorize the ultrasonic stress-strain field might follow the pressure sphere of influence, specifically taking the shape of a bell curve. Any interface underneath the ultrasonic stress-strain field would

Figure 9 Results from FEA model showing progression of 95°C plane front of heat

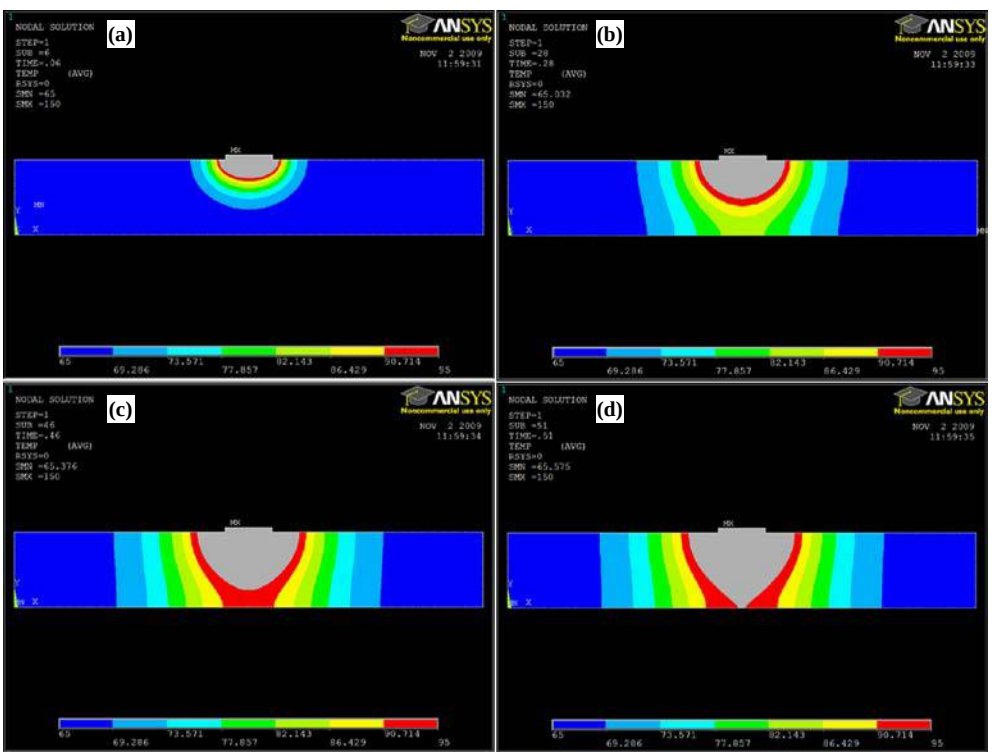

Notes: (a) At 0.06 seconds, the plane reached one-fourth through the build; (b) at 0.28 seconds, the plane reached half through the build; (c) at 0.46 seconds, the plane reached three-fourth through the build; (d) at 0.51 seconds, the plane reached the bottom of the build

Figure 10 Actual time of maximum temperature for 65°C block weld five thermocouples plotted with theoretical time of peak temperature based on the FEA model

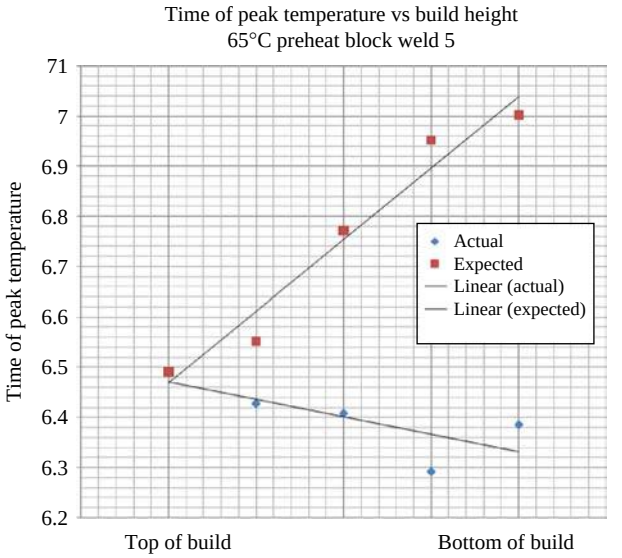

Figure 11 Schematic representation of the ultrasonic stress-strain field

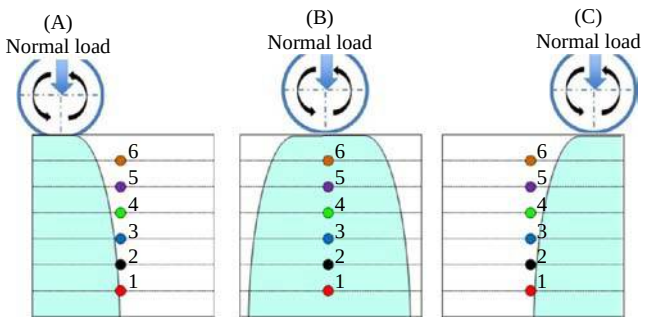

Note: It is purposed the ultrasonic energy will be dissipated at all interfaces underneath the pressure sphere of influence of the sonotrode

absorb some of the ultrasonic energy and convert it locally to heat. This will be important for future research programs attempting to model UAM as heat is generated throughout the build, not just on the topmost interface.

3.5. Calculated temperature rise

In order to estimate the actual power absorbed at the topmost interface (the foil above and below the thermocouple), equation (2) was used. It was calculated for the highest recorded temperature increase, 109°C, 2.9 per cent of the total powerinput (3 kW) was absorbed at the topmost interface. The calculated temperature rise of the topmost thermocouple versus different efficiencies is presented in Table V. It has been estimated that the overall process efficiency (power input absorbed and converted to heat by the build) is approximately 30 per cent. This indicates that only 10 per cent of the total absorbed power is absorbed in the topmost interface, while 90 per cent is absorbed lower in the build. Finally, using the 30 per cent overall efficiency, it was possible to solve for the interaction volume of the ultrasonic stress-strain field.

Table V Theoretical temperature rise of first interface given a percentage of the total power absorbed there

Efficiency (%)	Energy input (w/mm^3)	Heat input (J/mm^3)	Temperature rise (°C)
2.90	2.81	0.27	109
5	4.92	0.47	191
10	9.8	0.93	382
30	29.5	2.8	1,146

It was estimated that the temperature increase of the material was a constant 35°C and the ultrasonic stress-strain field was approximated as a rectangle with two sides known (25.4 mm sonotrode width and 8.25 mm build height). It was found the overall interaction volume was approximately 1,000 mm^3 yielding a length of interaction beneath of the sontrode of 4.8 mm in the travel direction. This approximation results in a plane of heat generated beneath the sonotrode.

3.6. Cooling coefficient analysis

Analyzing the data with equation (1) revealed heat was dissipated away from the weld zone at a surprisingly low rate, with the effective thermal diffusivity usually <1 per cent of the expected value for aluminum 3003 (Figure 12). While there is some scatter in the data, it is clear the thermal diffusivities calculated here are much lower than bulk aluminum, indicating slower than normal bulk aluminum cooling is occurring. The exact reason for this decreased cooling rate is unknown, though it is possibly linked to the voids and oxides found throughout the interfaces as well as the heat generated throughout the build. The major factor contributing to this is thermal contact resistance, where the flow of heat is restricted to only flowing through small asperity micro contacts, severely limiting the thermal diffusion across interfaces. The many separate layers that make up a UAM build, each with voids and potentially oxides present, increases the impact of the thermal contact resistance. With thermal diffusion across interfaces greatly diminished, the heat must be transfered along the plane of the interface and away from the sonotrode. However, as heat generated along interfaces throughout the build, no "cold" areas exist for the heat to flow to, slowing the cooling rate even further.

Figure 12 Results of the effective thermal diffusivity calculations

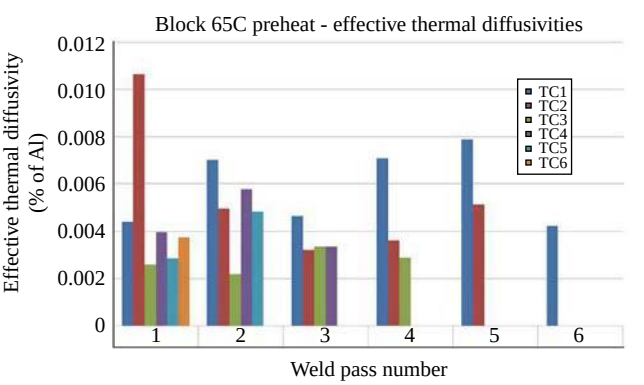

3.7. Solid block control experiment

The thermocouple results from the first welding pass of the block control experiment are shown in Figure 13. As expected, it was found there was a delay in time as the heat generated at the top of the build was conducted down to the lower parts. Lower thermocouples reported a longer delay before the beginning of heating, and did not heat as high as the upper thermocouples. The topmost thermocouple reported a maximum temperature of 75°C while the bottom thermocouple reported a maximum temperature of 70°C. These temperatures indicate a maximum temperature increase of 10°C above the preheat temperature, much less than the 25-35°C increase the lower thermocouples in the UAM build reported. This confirmation experiment proved the ultrasonics and pressures applied had no significant impact on the thermocouple readings of the earlier block and step builds. This supports the finding that ultrasonic energy is locally attenuated at each interface resulting in local heating of that interface.

4. Conclusions

The focus of this research program was to make *in situ*, accurate, temperature readings during the UAM process. The primary conclusions are:

- Heating and cooling patterns for all of the welding passes of the 65°C preheat builds and most of the 149°C preheat builds followed normal heating and cooling shapes. Maximum temperatures of 220°C were observed, well below the melting temperature of aluminum.
- Instantaneous heating and cooling rates of up to 3,000°C/s were recorded. The highest rates were recorded during the first welding pass when the thermocouple was first embedded and experienced the highest temperatures.
- A simultaneous heat generation at all interfaces was observed. This proves ultrasonic energy is transmitted and absorbed throughout the entire build, not just the topmost interface. However, as evidenced by the peak temperatures recorded, the topmost interface does absorb the most ultrasonic energy. The control experiment proved the ultrasonic energy and pressures applied do not artificially influence the thermocouple readings.
- An ultrasonic stress-strain field was proposed to account for the simultaneous heating observed. Ultrasonic energy is locally converted to heat under this stress-strain field. A rough approximation found the length of the ultrasonic stress-strain field (in the travel direction) was approximately 4.8 mm.
- Calculated effective thermal diffusivities averaged <1 per cent of the reported values for aluminum 3003. This indicates a severe hindrance to thermal diffusion, most likely due to voids and oxides at interfaces increasing the thermal contact resistance across the interfaces. For modeling purposes, it will be necessary to assume an effective thermal conductivity much lower than reported values in the literature for bulk aluminum.

Figure 13 Results of the solid block confirmation experiment

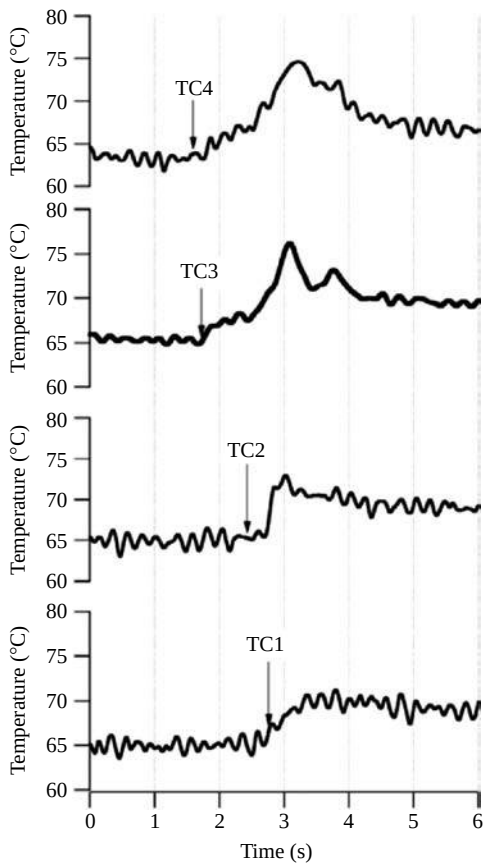

References

de Vries, E. (2004), "Mechanics and mechanisms of ultrasonic metal welding", PhD thesis, The Ohio State University, Columbus, OH.

Grong, O. (1997), *Metallurgical Modelling of Welding*, Ashgate, Surrey, pp. 80-2.

Grujicic, M., Zhao, C.L. and Dusel, E.C. (2005), "The effect of thermal contact resistance on heat management of the electronic packaging", *Applied Surface Science*, Vol. 246, pp. 290-302.

Gunduz, I.E., Ando, T., Shattuck, E., Wang, P.Y. and Doumandis, C. (2005), "Enhanced diffusion and phase transformations during ultrasonic welding of zinc and aluminum", *Journal of Acta Materialia*, Vol. 52, pp. 939-43.

Hatch, J.E. (1984), *Aluminum: Properties and Physical Metallurgy*, ASM International, Metals Park, OH, p. 92.

Hazlett, T.H. and Ambekar, S.M. (1970), "Additional studies of interface temperature and bonding mechanisms of ultrasonic welds", *Welding Journal*, Vol. 49 No. 5, pp. 196-200.

Janaki Ram, G.D., Robinson, C., Yang, Y. and Stucker, B.E. (2007), "Use of ultrasonic consolidation for fabrication of multi-material structures", *Rapid Prototyping Journal*, Vol. 13, pp. 226-35.

Johnson, K. (2008), "Interlaminar subgrain refinement in ultrasonic consolidation", PhD thesis, Loughborough University, Loughborough.

Kong, C.Y., Soar, R.C. and Dickens, P.M. (2004a), "A model for weld strength in ultrasonically consolidated

components", *Journal of Mechanical Engineering Science*, Vol. 219, pp. 83-91 (Part C).
Kong, C.Y., Soar, R.C. and Dickens, P.M. (2004b), "Ultrasonic consolidation for embedding SMA fibers within aluminum matrices", *Composite Structures*, Vol. 66, pp. 421-7.
Li, D. and Soar, R.C. (2008), "Plastic flow and work hardening of Al alloy matrices during ultrasonic consolidation fiber embedding process", *Materials Science & Engineering A*, Vol. 498, pp. 421-9.
Weare, N.E., Antonevich, J.N. and Monroe, R.E. (1960), "Fundamental studies of ultrasonic welding", *Welding Journal*, Vol. 39 No. 8, pp. 331-41.
Yang, Y., Janaki Ram, G.D. and Stucker, B.E. (2007), "An experimental determination of optimum processing parameters for Al/SiC metal matrix composites made using ultrasonic consolidation", *American Society of Mechanical Engineers*, Vol. 129, pp. 538-49.
Yang, Y., Janaki Ram, G.D. and Stucker, B.E. (2009), "Bond formation and fiber embedment during ultrasonic consolidation", *Journal of Materials Processing Technology*, Vol. 209, pp. 4915-24.

About the authors

David Schick received a Bachelor's of Science in Welding Engineering from the OSU in 2008 as part of a BS/MS program. He received a Master's of Science under Sundarsanam Suresh Babu and John C. Lippold studying ultrasonic additive manufacturing in December 2009.

Sudarsanam Suresh Babu is an Associate Professor in the Welding Engineering Program of the Integrated Systems Engineering Department of OSU. Before joining OSU, Dr Babu served as a Technology Leader of Engineering and Materials in Edison Welding Institute, North America's premier research and development organization related to materials from 2005 to 2007. Before 2005, Dr Babu held positions as a Senior Research Staff Member at Oak Ridge National Laboratory (ORNL), and joint positions between ORNL, University of Tennessee, Penn State University, as well as the National Institute of Materials Science, Japan. Suresh obtained his Bachelor of Engineering degree from PSG College of Technology, Coimbatore, India and Masters degree in Industrial Metallurgy from Indian Institute of Technology, Chennai, India. He obtained his PhD in Materials Science and Metallurgy from University of Cambridge, Cambridge. Sudarsanam Suresh Babu is the corresponding author and can be contacted at: babu.13@osu.edu

Daniel R. Foster is a PhD student in the Mechanical Engineering Department at the OSU. He is a Member of the Smart Materials and Structures Laboratory investigating the "fundamentals of ultrasonic additive manufacturing".

Marcelo Dapino is an Associate Professor of Mechanical Engineering and Director of the Smart Materials and Structures Laboratory, a facility dedicated to the study of smart materials, coupled dynamic systems, mechanical design, and control engineering. As author of over 120 technical articles, Professor Dapino has made substantial scientic and applied contributions through his work on automotive, aerospace, biomedical, and naval applications from a comprehensive viewpoint encompassing experimental, analytical, and computational research. Professor Dapino is a core investigator on multiple research programs sponsored by industry and government agencies, including among others an Office of Naval Research Multidisciplinary University Research Initiative on iron-based magnetostrictive alloys, a National Science Foundation Industry/University Collaborative Research Center on smart vehicle concepts (for, which he is an Associate Director), a Third-Frontier Wright Project on high power ultrasonic additive manufacturing, and the Honda/OSU Multidisciplinary Innovation Exchange (as the OSU Coordinator). Professor Dapino serves as a Co-chair of the Adaptive Structures and Material Systems Technical Committee of the American Society of Mechanical Engineers and has served as a Lead Organizer of several international conferences on smart materials.

Matt Short joined EWI in 2004, bringing a diverse background in ultrasonic joining systems, custom tooling, and automation. In his current role as a Engineering Team Leader, he continues to focus on the expanded uses of high-power ultrasonics in additive manufacturing, welding and machining, as well as having responsibility for building EWI's, technical expertise in the technology and applications of ultrasonics.

John C. Lippold, PhD, is a Professor in the Welding Engineering Program at the OSU and a Leader of the Welding and Joining Metallurgy Group. A Fellow of both the American Welding Society and ASM International, Dr Lippold has received numerous awards, including the Charles H. Jennings Memorial Award, the William Spraragen Memorial Award, the Warren F. Savage Memorial Award, the McKay-Helm Award, the A.F. Davis Silver Medal, the James F. Lincoln Gold Medal, the William Irrgang Memorial Award, and the Dr Comfort A. Adams Lecture Award.

This article has been cited by:

1. Niyanth Sridharan, Paul Wolcott, Marcelo Dapino, S.S. Babu. 2016. Microstructure and texture evolution in aluminum and commercially pure titanium dissimilar welds fabricated using ultrasonic additive manufacturing. *Scripta Materialia* **117**, 1-5. [CrossRef]
2. R.J. FrielPower ultrasonics for additive manufacturing and consolidating of materials 313-335. [CrossRef]
3. Justin J Scheidler, Marcelo J Dapino. 2013. Nonlinear dynamic modeling and resonance tuning of Galfenol vibration absorbers. *Smart Materials and Structures* **22**:8, 085015. [CrossRef]